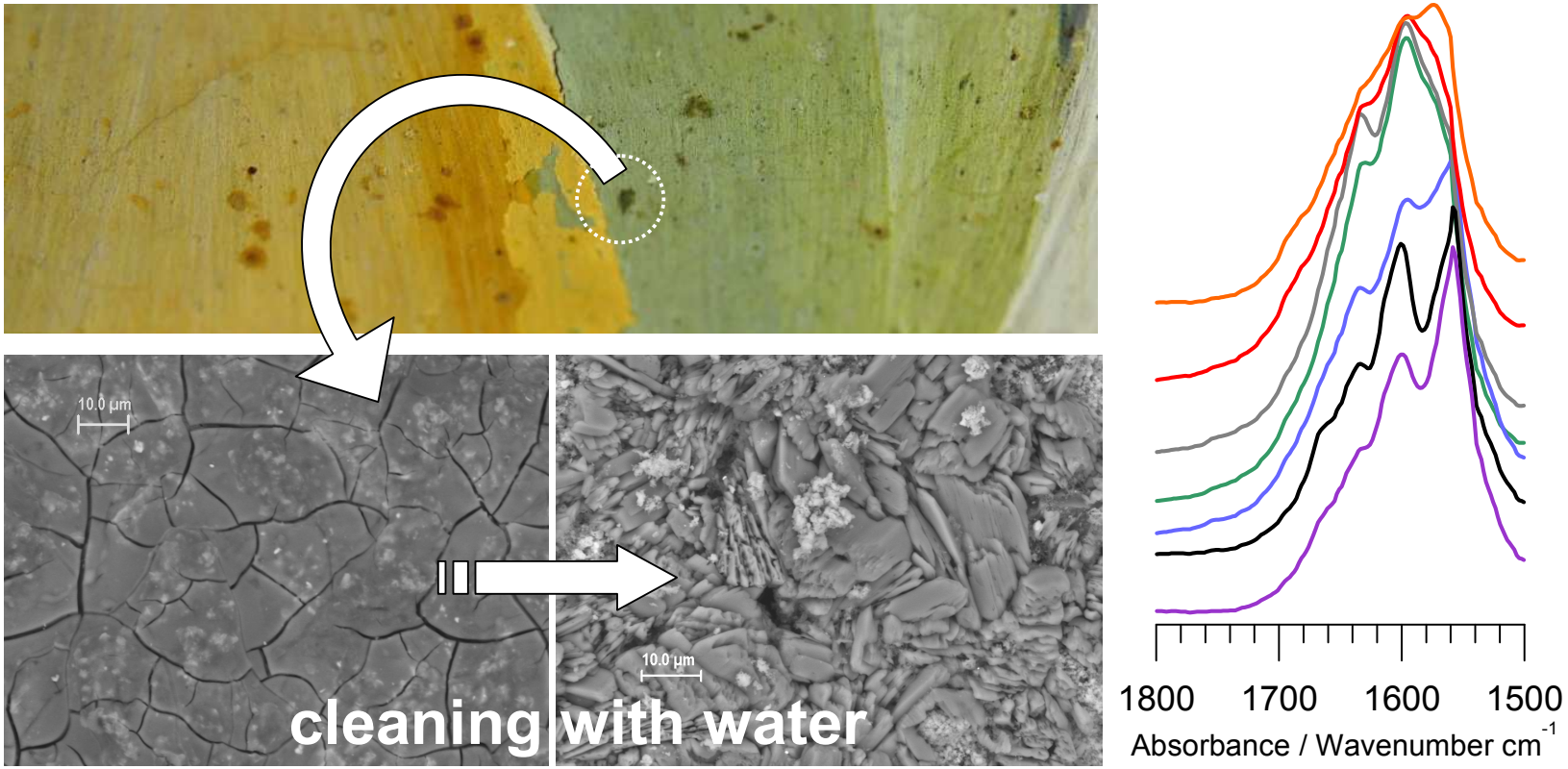
10.0 µm
10.0 µm
cleaning with water
1800
1700
1600
1500
Absorbance / Wavenumber cm-1

LOW MOLECULAR WEIGHT ORGANIC ACID SALTS, MARKERS OF OLD FUNGI ACTIVITY IN WALL PAINTINGS

Nati Salvadó[1,2*], Salvador Butí[1,2], Trinitat Pradell[2,3], Victòria Beltran[1,2], Gianfelice Cinque[4], Jordi Juanhuix[5], Lídia Font[6], Rosa Senserrich[7].

1. Dpt. d'Enginyeria Química. EPSEVG. Universitat Politècnica de Catalunya, Av. Víctor Balaguer s/n, 08800 Vilanova i la Geltrú, Barcelona
2. Center for Research in Nano-Engineering, Universitat Politècnica de Catalunya, Barcelona, Spain
3. Dpt. Física. Universitat Politècnica de Catalunya. Campus del Baix Llobregat, c. Esteve Terradas 8, 08860 Castelldefels, Barcelona
4. Diamond Light Source, Harwell Campus, Chilton-Didcot OX11 0DE Oxon, U.K.
5. CELLS-ALBA Synchrotron, Ctr. BP 1413, de Cerdanyola a Sant Cugat, km 3,3, 08290 Cerdanyola del Vallès, Barcelona
6. Museu d'Historia de Barcelona MUHBA, Institut de Cultura, Ajuntament de Barcelona, Llibreteria 7 4t, 08002 Barcelona
7. Secció de Conservació i de Restauració de la Facultat de Belles Arts, Universitat de Barcelona, Pau Gargallo 4, 08024 Barcelona

* Corresponding author:
E-mail address: nativitat.salvado@upc.edu
Telephone: 0034938967717
Fax: 0034938967700

Keywords: low molecular weight organic acids, filamentous fungi, infrared spectroscopy, cultural heritage, microanalysis, synchrotron light

Abstract

Micro Infrared Spectroscopy (µSR-FTIR) and X-Ray diffraction (µSR-XRD) with synchrotron light, Gas Chromatography/Mass Spectrometry (CG/MS), Optical Microscopy (OM) and Scanning Electron Microscopy (SEM/EDS) were used to identify and obtain the distribution of complex mixtures of calcium salts of low molecular weight organic acids (LMWOA) in micro-layered micro-samples. Filamentous fungi produce LMWOA that can react with metal cations producing stable salts. These substances were found in the dark spots covering the surfaces of Saint Michael's Chapel wall paintings of the Royal Monastery of Pedralbes in Barcelona linking them to old fungi activity. The presence of glycerol likewise related to the fungi activity is also identified in the layers.

1. Introduction

Fungi attacks are a frequent problem in paintings and, generally speaking, are not easily diagnosed as very often the fungi are not any longer active [1-5]. Fungi develop from spores transported by the air which, if the humidity and temperature are favourable to their growth, germinate on the walls surface. Fungi are rarely tied to a

specific substratum and the same species can be found on surfaces as different as wall paintings or leather [2]. The most common types of the fungi found on wall paintings in either the warmest or most temperate climates are, among others, *Aspergillus, Penicillium, Cladosporium* and *Alternaria* [2,3]. During their period of activity fungi produce a large variety of secretion substances which react with the environment or the paintings producing other compounds. If the atmospheric conditions are unfavourable to the fungi development, they die and all the substances resulting from the bioactivity also decompose and disappear remaining only those which are more stable. In the case of ancient wall paintings the fungi activity could have taken place a long time ago, even centuries ago, but still the most stable reaction products are likely to be found.

Among other substances fungi produce organic acids of low molecular weight (LMWOA) such as lactic, citric, oxalic, succinic, glutamic, fumaric, malic or acetic acids, mostly related to the reactions happening in the Krebs cycle [1,2]. Some of these acids or the corresponding salts produced by their reaction with metal cations are relatively stable. Calcium oxalates, for example, are found on many surfaces, although their origin is diverse and, consequently, they cannot be considered as an indicator of fungi activity. On the contrary, the presence of salts from malic, fumaric or succinic acids is directly related to the existence of old fungi activity.

The dark spots covering the surfaces of wall paintings were presumed to be the remnants of old fungi activity, as the distribution did not show any relationship with the substratum. The pictorial decorations of Saint Michael's Chapel studied are situated in the cloister of the Royal Monastery of Pedralbes in Barcelona[6] and were carried out in 1346 (**Fig. 1**). They have been long attributed to the painter Ferrer Bassa, to whom, according the documentation, was commissioned the work by the abbess of the monastery. The paintings are in a good state of conservation although some alterations are evidenced. The paintings are currently being restored[7], and the present study is part of a comprehensive program of Restoration. The study of the chemical nature of the dark spots is essential to design a plan for restoration that is effective as well as respectful for the pictorial layers.

The small thickness of the layers formed by the fungi activity (between 10-15 micrometres thick), the small amount of sample material available for analysis, as well as, the variable proportions in which the fungi related compounds are present in the layers, strongly difficult and limit their identification. Moreover, the various degrees of hydration of the crystals and the potential possibility of mixed salts formation also add to the difficulty of their identification. Finally, other materials such as silicates, gypsum, calcium carbonate and other organic materials either from environmental pollution (dust) or from the burning of candles are also often deposited on the surfaces and appearing in the layers.

Samples extracted from the paintings were analysed by means of Optical Microscopy (OM), Scanning Electron Microscopy (SEM/EDS), Micro Infrared Spectroscopy (µSR-FTIR) and Micro X-Ray diffraction (µSR-XRD) with synchrotron light and Gas chromatography–mass spectrometry (GC-MS). The combination of these analytical

techniques can overcome the analytical challenge and provide essential information about the old fungi activity leading to a better understanding of the relationship between fungi and the paint substratum. Infrared spectroscopy was used as a first step in the identification of the nature of those substances and the LMWOA anions were determined using the whole of a sample using GC-MS. Their distribution in the layers was resolved using the micro-analytical techniques[8,9]. Synchrotron radiation (SR) thanks to the high brilliance, energy selection and collimation of the beam enables obtaining spectra with a very high signal to noise ratio on areas as small as a few micrometres. In particular, the high selectiveness of the small spot analysed compensates the relatively low detection limit of FT-IR (about 10% of the measured area) and the relatively low sensitivity of XRD (between 1-5% depending on peak overlapping), helping to determine compounds present in extremely small amounts from a few microgram samples. This aspect becomes particularly important for fragments taken from an artwork. It is worth to highlight that the new generation of portable XRD and IR equipment might facilitate sampling the artworks, either identifying original materials or the kind of alterations under study, thanks to their non-destructiveness. However, they will hardly be a substitutive of SR based micro-analytical techniques as they cannot produce the high quality data necessary. Laboratory based micro-analytical techniques although showing a great potential in cultural heritage studies, often, either are not able to collimate the beam down to the spot size adequate (FTIR) or the brilliancy of the beam is not high enough to obtain the data quality required to determine the compounds (XRD).

2. Materials and methods

Synthesis of calcium salts: The synthesis of the LWMOA calcium salts was produced by stoichiometrically mixing the necessary amount of acid and calcium hydroxide or calcium carbonate with water, homogenized and afterwards dried by evaporation of the water at 25°C. Reagents: DL-Malic ($COOH-CH_2-CH_2-COOH$), Fumaric ($HO_2CCH=CHCO_2H$) and Succinic ($HOOC-CH_2-CH_2-COOH$) acids were purchased from TCI; Lactic acid ($H_3C-CH(OH)-COOH$), calcium carbonate $CaCO_3$ and calcium hydroxide $Ca(OH)_2$ were purchased from Panreac; Calcium Lactate pentahydrate $Ca(H_3C-CH(OH)-COO)_2{\cdot}5H_2O$ and calcium oxide CaO were purchased from Sigma Aldrich.

Optical Microscopy (OM): Microsamples were manipulated under a Stereomicroscope, SMZ800 Nikon. Fragments, sections and thin slices were observed with an Optical microscope Eclipse LV100 Nikon. Polished cross sections and thin preparations were prepared embedding the samples in epoxy resin and subsequent microtoming. For some samples, and with the aim of avoiding the contamination of the most superficial layers, they were previously coated with a thin gold protecting layer before embedding them in epoxy resin.[8]

Infrared spectroscopy:

µSR-FTIR measurements were taken at beamline MIRIAM B22 of the Diamond Light Source, UK[10]. The Bruker 80 V Fourier Transform IR Interferometer is equipped with Hyperion 3000 microscope, a broad-band high sensitive MCT detector and a 36x condenser. The spectra were obtained in transmission mode using a small beam spot of 15x15 square microns, 4 cm^{-1} resolution, co-adding 256 scan at scanner velocity 80 kHz (35 sec), in the 4000 to 650 cm^{-1} wavenumber range. IR maps of the molecular composition were obtained by scanning the sample via a micrometric resolution motorized X-Y stage. Selected sample fragments were squeezed between two diamonds into an anvil cell to obtain samples of adequate thickness and to spread and separate the different substances.

FTIR spectra of reference salts were measured with a Shimadzu IRAffinity-1, 4 cm^{-1} resolution, 128 scans, in the 4000 to 400 cm^{-1} wavenumber range. The analysis was performed using KBr pellets (13 mm diameter).

X ray diffraction: Synchrotron based micro-X-ray diffraction patterns (µSR-XRD) were obtained from samples extracted from the artworks at beamline XALOC of the ALBA Synchrotron, Cerdanyola del Vallès (Barcelona). 20 µm thick microtomed cross sections of the samples were measured with a focused beam of 50x6μm^2 (FWHM), 1s acquisition time and 12.6 keV energy in a virtually noise free Pilatus 6M (Dectris) detector with a large (424x435 mm^2, 6 Mpixels) active area[11]. The diffraction patterns from all the layers were obtained by scanning the sample over ca. 150 µm with a step of 6 µm.

Scanning Electron Microscope: Fragments, sections and thin slices were observed by means of a GEMINI SEM equipment with a Shottky-FE column at 4pA-20 nA, 0.1 to 30 kV and 1nm resolution for 20KV. Elemental analysis was made with an EDS with an INCAR Penta FETX3 detector and a 30 mm^2 ATW2 window.

Gas chromatography /mass spectrometry: GC-MS, 5975C Series GC/MSD System - Agilent Technologies, Agilent 6850, column HP-5MS. The samples were dissolved in an excess of derivatization reagent (50 µl de BSTFA) heated up to 70^oC for 3 hours. Working conditions were splitless injection and a nonlineal heating rate from 40 to 300^oC. The identification of the molecules was made comparing with a NIST 2 database.

3. Results and discussion

Small dark spots (occupying a surface of few millimetres in size) randomly distributed on some areas of the wall paintings are observed. At the beginning of this study their nature was not clear, so their chemistry had to be determined to assert their origin and to obtain information about their composition necessary for an adequate restoration (removal). The spots were present all over the paintings indistinctly of the nature of the substratum, appearing over different colour paints and materials, but being more visible in the lighter tones. In this study samples from different areas of the paintings with different base colours were analysed.

In the areas affected, alongside the dark spots, crystal growths of an ochre colour are sporadically observed. A blue coloured area affected by those grows is shown in **Fig. 2 and 3**. The crystal growths (**Fig. 2a**) contain a large proportion of calcium oxalates as well as a residual presence of protein and carbohydrate (**Fig. 2b**). Moreover, up to 100 µm long and ~1,5 µm wide filaments containing carbohydrate are also sporadically observed. Both the crystal growths and the filaments are most probably related to old filamentous fungi[12-14]. The spots appear shiny and show a smooth surface (**Fig. 3a**). SEM-EDS analyses of the dark spots reveal the presence of calcium as the only metal element present.

This old fungi activity is responsible for the presence of fungi secretion~~s~~ substances that still persist as well as, of the corresponding reaction compounds of those secretions. Although, the identification of the nature of the substances is essential, it is even more important to determine the degree of affectation of the painting and, consequently, confirm their presence in the most internal layers of the paint. For this reason, cross sections of the samples were prepared and the different paint layers analysed. **Fig. 3b,c,d** show the cross section corresponding to a blue paint. The Scanning Electron Microscopy (SEM) image from the cross section of the sample (**Fig. 3c**) shows the presence of a layer formed by large (5-10µm) very characteristic blue pigment particles of azurite, $2CuCO_3{\cdot}Cu(OH)_2$. The most external surface of the paint layer shows a continuous thin brownish film covering (10 and 15 µm thick) the irregular shape of particles which contains only one metallic element, calcium (**Fig. 3d**).

A fragment of the same blue painting was squashed and the various paint layers (see **Fig.4a**) spread on a diamond cell keeping the layered structure as shown in **Fig.4b**. The thickness of the layers is such that may be analysed in transmission mode by infrared spectroscopy. The corresponding µSR-FTIR spectra are shown in **Fig. 4c**. The inner black layer contains calcium carbonate and calcium oxalates (carbon, the most likely black pigment, cannot be detected by infrared spectroscopy). The spectrum of the blue layer confirms the presence of azurite particles seen in the SEM image **(Fig.3c**). Finally, the spectra corresponding to the most external brownish layer are very similar and suggest a homogeneous mixture of calcium salts of low molecular weight organic acids (LMWOA salts). The IR spectra of those substances show characteristic main bands of organic salts, namely the asymmetric and symmetric stretch vibrations of the deprotonated carboxylate groups and the stretching and bending bands from the νOH group. Stretching and bending of C-H groups can also be observed but with a low intensity due to their low molar absorptivity.

In order to confirm the family of substances as well as the anions present, a fragment of the paintings was subjected to Gas Chromatography–Mass Spectrometry (GC-MS). In particular, succinic, fumaric, malic and lactic acids are determined which are known to be secreted in variable proportions by various fungi species[15,16]. Moreover, among them, glycerol was also determined; glycerol can be produced by some species of fungi when stressed by water shortage[2].

It is also very important to notice that these calcium LMWOA salts are determined by µSR-FTIR only in the most external brownish (**Fig. 4**); in contrast, the calcium oxalates

are present also in the internal layers, as is shown in **Fig. 5**. Oxalates are known to form by the degradation of the binding medium (protein binder). The painting technique used in these wall paintings combines *fresco* (calcium carbonate binder) with *secco* (which involves the addition of an organic binder) and, consequently, the calcium oxalates present in the inner paint layers could result from the degradation of the organic binder.

Noteworthy, some of these LMWOA salts formed are crystalline enough to be determined by x-ray diffraction (µSR-XRD), **Fig. 6**. **Fig. 6a** shows the µSR-XRD pattern from the layer related to old fungi activity, which was detached from a blue paint layer. In this case, two different crystalline LMWOA salts are determined, confirming the presence of more than one LMWOA salts in the brown spots. One of them could be identified as calcium malate dihydrate (JPDF file 00-030-1575)[17]. The second compound could not be related to any of the patterns found either in the literature or among those sintered by us.

Moreover, the µSR-XRD patterns corresponding to a microtomed cross section of one sample extracted from an ochre paint are shown in **Fig. 6b**. Two layers are observed; the ochre paint below and a most external layer containing the substances related to old fungi activity on top. The ochre paint is essentially a clay containing goethite - FeO(OH)- , quartz –SiO_2-, calcite –$CaCO_3$-, weddellite –calcium oxalate dehydrate, $CaC_2O_4{\cdot}2H_2O$- and bassanite –calcium sulphate hydrate, $CaSO_4{\cdot}0.5H_2O$- which has broad peaks and, consequently, low crystallinity, also in good agreement with the composition of an ochre clay, magnesium, aluminium, silicon, sulphur, potassium, calcium and iron. The µSR-XRD pattern corresponding to the most external layer shows the same unknown crystalline compound found in the blue paint and some calcite; this is in good agreement with the fact that calcium, together with some chlorine related to atmospheric contamination is the main compound determined by SEM-EDS analysis (**Fig.6c**).

The small thickness of the microtomed cross section of the samples together with the small size and high brilliance of the beam have been crucial to obtain distinct µSR-XRD patterns of the crystallites related to the fungi activity considering the low intensity of the diffraction patterns of the salts and the small thickness of the layers formed.

Both infrared spectra and x-ray diffraction patterns obtained from different samples corresponding to different substrata and painting colours show how these substances are present in various proportions in all the dark spots. The fact that the infrared spectra and XRD patterns obtained do not coincide exactly with the reference data available in the literature[17-19] or with the LMWOA salts sintered by us (**Fig. 7**), may be explained by the extreme complexity of the layers found in the paintings: mixed LMWOA salts showing different degrees of hydration and which are also present in various proportions. **Fig. 8**. The salts identified correspond to calcium salts of the monocarboxylic and dicarboxylic acids where the anions act as monodentate, bidentate or tridentate ligands[20,21]. Moreover, their stability and crystallinity depend also on the presence of hydration water[22]. Oxalate, malate, lactate, succinate, fumarate can show various degrees of hydration (polihydrated salts) with different crystalline growth habits or even also often amorphous halos. For this reasons, an

extensive database of low molecular weight organic acid salts is being elaborated in order to identify, in the near future, the specific chemical species.

Despite this lack of complete information, a tentative interpretation of the complex infrared spectra (**Fig. 8**) is proposed. The 3800-2500 cm^{-1} region of the infrared spectra of the compounds identified in the paint samples is shown in **Fig. 8b**. This region includes many bands (some overlapping each other) corresponding to (O-H) stretching vibrations of –OH groups which may be found in many different ways. The alcohol groups show bands at ~3600 cm^{-1} for the free –OH, at ~3550 cm^{-1} for the intramolecular bonded –OH, at 3400-3200 cm^{-1} for the intermolecular –OH bonds and below 3200 cm^{-1} for the chelated groups. Carboxylic groups show bands between 3560-3500 cm^{-1} for the free –OH groups and between 2700-2500 for the bonded –OH groups. Finally, in this region, hydrogen bonds related to vibrations from both, hydroxyl groups and water molecules (crystallization water in the salts can form strong hydrogen bonds) are also seen[23,24]. The 1800-600 cm^{-1} region of the infrared spectra is shown in **Fig. 8c**. The 1630 cm^{-1} band is difficult to assign, as although it could be assigned to the alkenyl C=C stretching found in the fumarate salt it is also present in the succinate salt reference spectrum (**Fig 7**) related to the δ(O-H) bending mode of H_2O [20]. C=O asymmetric stretching vibration bands of the carboxylate group (carboxylic acid salt) are found in the interval between 1550 and 1600 cm^{-1}. The bands observed at 1427 or 1440 cm^{-1} can be associated to the C-O symmetric stretching vibration of the carboxylate group[11], but also to the δCH_2 mode of methylene group[18,25] (a small contribution due to the presence of carbonate, calcium carbonate, cannot be fully withdrawn). The bands observed at 1391 and 1409 cm^{-1} can be related to the CH_3 asymmetric bending vibration (present in the lactate salt), but also to the C-O symmetric stretching vibration of the carboxylate group[18,25]. The band observed between 1340 and 1350 cm^{-1} can be associated to the wagging of the CH_2 methylene group or to the CH_3 symmetric bending vibration (present in the lactate salt). The sharp bands at 1051 and 1103 cm^{-1} might be related to the C-O- stretching of the primary and secondary alcohols, respectively. However, at 1051 cm^{-1} a band is also found in the calcium malate reference spectrum although calcium malate does not contain primary alcohols. The bands observed at 892 or 813 cm^{-1} can be attributed to the rocking and wagging modes of water molecules. And finally the band centred at 690 cm^{-1} can be related to the calcium oxygen, νM-O, stretching vibration; although it also overlaps with other bands such as the δ(OCO) band.

A high quality spectrum is required to discriminate the presence of the LMWOA salts from other compounds. For instance, **Fig. 9** shows how a green earth pigment, such as celadonite (3602, 3558, 3535 cm^{-1}) [26-28] showing bands in the νOH region very close to those corresponding to the salts from secreted organic acids, may disturb the correct identification of the LMWOA salts. This example highlights the need of high quality infrared spectra to discriminate those substances in the paint samples; something that requires a particularly accurate preparation and manipulation of the samples.

One of the most remarkable characteristics of those layers related to old fungi activity is that water rinsing of the dark spots is able to remove completely the brownish-

yellowish substance associated to the crystallites which became afterwards translucent colourless. The resulting colourless crystals are the salts of low molecular weight organic acids analysed so far. Furthermore, the analysis of the brown residue extracted shows, apart from the presence of calcium carbonate and carbohydrates dragged in the water cleaning process, a water soluble dark brown pigment with absorption bands at ~3400, 2930, ~1590, ~1390 cm^{-1} which may be related to a melanin pigment[29]. Melanins are blackish brown pigments present in animals, plants, bacteria and fungi to protect them mainly from the UV radiation. In fungi, melanin is an important protective factor against the adverse effects of environmental stress, such as UV radiation, drying periods or presence of high concentrations of salts. In general, the chemical structure of melanins is still not completely understood because they are complex polymers of amorphous nature. Most groups of melanins are water insoluble. A exception are pyomelanins (included in the allomelanin group), which are water soluble and may be secreted by filamentous fungi[29,30].

The dark brown colour of the spots heavily affects the appearance and readability of the paintings, but their removal can only be obtained using specific chemicals which may also affect the integrity and stability of the paintings. The translucent colourless LMWOA salts left after removal of the brown pigment are relatively invisible and therefore, affect in a very limited form the appearance of the paintings. Therefore, and considering that the removal of the brown colourant substance is very simple and undamaging, it is advisable to proceed by removing it but leaving the LMWOA salts.

4. Conclusions

Calcium LMWOA salts have been determined in the dark spots localised on the surface of 14th century wall paintings. In particular, calcium salts of the oxalic, malic, lactic, succinic and fumaric acids. Those salts are directly related to the reaction compounds of the acids secreted by fungi and the environment depositional calcium compounds. Those substances appear forming a thin, 10-15 µm thick, superficial layer and show little interaction and low penetration within the painting layers.

Both infrared spectra and x-ray diffraction patterns obtained from different samples corresponding to different substrata show that those fungi layers contain various proportions of salts showing different degrees of hydration and crystalline growth habits.

In the context of paintings conservation, revealing the nature of those substances that form the dark spots has pointed out the difficulty of fully eliminating them without affecting the paint layers. The dark colour shown by those affected areas is, however, not due to the presence of these substances itself but to the presence of a brown colourant (possibly melanine secreted by the fungi), which is water soluble, and therefore, can be easily removed but leaving the colourless translucent LMWOA salts which do not affect the readability of the paintings. This treatment has been successfully applied in the restoration of the Saint Michael's chapel wall paintings.

Finally, the data obtained in this study has given enough analytical information about those substances to be able to determine their presence in other artworks using

portable or conventional laboratory equipment, which would have been very unlikely possible beforehand.

Acknowledgments

The project received financial support from MINECO (Spain), grant MAT2013-41127-R and Generalitat de Catalunya, grant 2014SGR-581. We acknowledge DIAMOND LIGHT SOURCE for time on Beamline MIRIAM B22 under Proposal (SM10400) and the collaboration of DIAMOND staff. The µSR-XRD experiments were performed at BL13 XALOC beamline (Grant No. 2014071016) at ALBA Synchrotron with the collaboration of ALBA staff.

This work is a part of the Restoration and Conservation Project of the Saint Michael's Chapel made by the "Institut de Cultura" of "Ajuntament de Barcelona" by means of the "Museu de Historia de Barcelona (MUHBA)" and the Royal Monastery of Pedralbes (Barcelona) directed by Lídia Font Pagès.

References

1 J. Karbowska-Berent, Microbiodeterioration of mural paintings: A review. In: R. J. Koestler, V. H. Koestler, A. E. Charola, F. E. Nieto-Fernandez (Ed.), *Art, Biology, and Conservation: biodeterioration of works of art*, The Metropolitan Museum of Art, New York, 2003, pp 266-301.

2 M-L. E. Florian, *Fungal facts: solving fungal problems in heritage collections*, Archetype Publications Ltd., London, 2002 (reprinted 2004).

3 O. Ciferri, *Appl. Environ. Microbiol.,* 1999, **65**(3), 879-885.

4 O. Pepe, L. Sannino, S. Palomba, M Anastasio, G. Blaiotta, F. Villaani, G. Moschetti, *Microbiol. Res.*, 2010, **165**, 21-32.

5 T. Rosado, M. Gil, A.T. Caldeira, M.R. Martins, C. Borrocas Diaz, L. Carvalho, J. Miräo, A. Estêväo Candeias, *Int. J. Archit. Herrit*., 2014, **83**, 85-852.

6 http://monestirpedralbes.bcn.cat/ca/monestir

7 L. Font, R. Senserrich, *The conservation of the paintings in Saint Michael's Chapel in the Monastery of Saint Mary of Pedralbes. Conserving Trecento Mural Paintings*. L. Font. (Ed.), MUHBA Documents **9**, Barcelona, 2014, pp. 71-104.

8 V. Beltran, N. Salvadó, S. Butí, G. Cinque, K. Wehbe, T. Pradell, *Anal. Chem.,* 2015, **87**, 6500-6504.

9 E. Pouyet, B. Fayard, M. Salomé, Y. Taniguchi, F. Sette, M Cotte, *Heritage Science*, 2015, **3:3**, 3-16.

10 G. Cinque, M. Frogley, K. Wehbe, J. Filik, J. Pijanka, *Diamond Synchrotron Radiation News*, 2011, **24**, 24-33.

11 J. Juanhuix, F. Gil-Ortiz, G. Cuni, C. Colldelram, J. Nicolas, J. Lidon, E. Boter, C. Ruget, S. Ferrer, J. Benach, *J. Synchrotron Radiat*., 2014, **21**, 679-689.

12 A. Szeghalmi, S. Kaminskyj, K.M. Gough, *Anal. Bioanal. Chem*., 2007, **387**, 1779-1789.

13 K. Jilkine, K. M. Gough, R. Julian, S. Kaminskyj, *J. Inorg. Biochem*., 2008, **102**, 540-546.

14 S. Kaminskyj, K. Jilkine, A. Szeghalmi, K. Gough, *FEMS Microbiol. Lett*., 2008, **284**, 1-8.

15 N. Liaud, C. Giniés, D. Navarro, N. Fabre, S. Crapart, I. Herpoël-Gimbert, A. Levasseur, S. Rauche, J.C. Sigoillot, *Fungal Biol. Biotechnol.*, 2014, **1**, 1-10.

16 J.K. Magnuson, L.L. Lasure, *Organic Acid Production by Filamentous Fungi. Advances in fungal Biotechnology for Industry, Agriculture and Medicine*. J. Lange, L. Lange (Ed.). Kluwer Academic/Plenum Publishers, 2004, pp. 307-340.

17 T. Jini, K. V. Saban, G. Varghese, *Crystal Research and Technology*, 2005, **40**(12), 1155–1159.

18 J. Thomas, A. Lincy, V. Mahalakshmi, K. V. Saban, *Crystallography Reports*, 2013, **58**, 93–97.

19 H. A. Bullen, S. A. Oehrle, A.F. Bennett, N. M. Taylor, H. A. Barton, *Appl. Environ. Microbiol*., 2008, **74**, 4553–4559.

20 M.P Binitha, P.P Pradyumnan, *Solid State Physics*, 2014, 1200-1202.

21 T. Jini, K.V. Saban, G. Varghese, S. Naveen, M.A. Sridhar, J.S. Prasad, *Journal of Alloys and Compounds*, 2007, **433**, 211–215.

22 Y. Sakata, S. Shiraishi, M. Otsuka, *Colloids and Surfaces B: Biointerfaces*, 2005, **46**, 135–141.

23 L. J. Bellamy, The infrared spectra of complex molecules, 3rd ed., Halsted Press, New York, 1975.

24 D. Lin-Vien, N. B. Colthup, W. G. Fateley, J. G. Grasselli, The Handbook of Infrared and Raman Characteristic Frequencies of Organic Molecules, Academic Press Limited, London, 1991.

25 A. Lincy, V. Mahalakshmi, J. Thomas, K.V. Saban, *IOSR Journal of Applied Physics (IOSR-JAP),* 2014, **6**(3 Ver. 1), 56-61.

26 G. S. Odin, A. Desprairies, P. D. Fullagar, H. Bellon, A. Decarreau, F. Frölich, M. Zelvelder, *Nature and geological significance of celadonite*. In: Green marine clays: oolithic ironstone facies, verdine facies, glaucony facies and celadonite-bearing rock facies—a comparative study, G. S. Odin (Ed.), Elsevier, Amsterdam, 1988.

27 C.A. Grissom, *Green earth*. In: Artists' Pigments, a Handbook of their History and Characteristics, vol. 1, R.L. Feller (ed)., National Gallery of Art, Washington, Archetype Publications Ltd., London, 1986 (reprinted 2012), pp. 141-167.

28 N. Salvadó, S. Butí, M.J. Tobin, E. Pantos, A.J.N.W. Prag, T. Pradell, *Anal. Chem.*, 2005, **77**, 3444-3451.

29 J. Schmales-Ripcke, V. Sugareva, P. Gebhardt, R. Winkler, O. Kniemeyer, T. Heinekamp, A.A. Brakhage, *Appl. Environ. Microbiol.*, 2009, **75**(2), 493-503.

30 N.N. Gessler, A.S. Egorova, T.A. Belozerskaya, *Appl. Biochem. Microbiol*., 2014, **50**(2), 125-134.

Figure captions:

Figure 1: 3D image of Saint Michael's Chapel from the Royal Monastery of Pedralbes (Barcelona). Vectorialized planimetry from Virginia Verdaguer with the help of Carla Puerto. Photography by Pere Vivas - MUHBA Archive.

Figure 2: Sample taken from a dark spot in a blue paint of the wall painting.

a) Optical microscopy image of the crystal growths protruding over the surface of the painting

b) µSR-FTIR spectra from the crystal growths: carbohydrate (1160-900 cm^{-1} region), protein (1650, ~1540 cm^{-1}) and calcium oxalate (1620 -overlapped-, 1323 cm^{-1}) are identified.

Figure 3: Sample taken from a dark spot in a blue area of the wall painting.

a) optical microscopy image from the surface.

b) optical microscopy image from a cross section of the sample

c) backscattered SEM image from the cross section

d) magnification of c) image, showing the 10 µm thick superficial layer related to old fungi activity.

Figure 4: Sample taken from the dark spot in a blue area of the wall painting

a) layers scheme corresponding to figure 3b image; 1: old fungi activity layer, 2: blue paint layer containing azurite particles, 3: calcium carbonate layer, 4: black substrate layer (calcium carbonate plus a black pigment) and 5: mortar (calcium carbonate plus sand)

b) optical image from a sample fragment squashed and spread keeping the layers structure on a diamond anvil cell. The corresponding µSR-FTIR spectra measured along the line marked are shown.

c) sequence of µSR-FTIR spectra from layer 3/4 to layer 1. Calcium oxalate is also determined in layer 4.

Figure 5: optical image from a sample fragment squashed and spread keeping the layers structure on a diamond anvil cell and the corresponding compounds distribution µSR-FTIR intensity maps obtained in transmission mode (rainbow colours). **a)** mapping of the 3429 cm^{-1}

band corresponding to azurite; **b)** mapping of the 875 cm^{-1} band related to calcium carbonate and **c)** mapping of the 1620 cm^{-1} band corresponding to calcium oxalate.

d) infrared spectra corresponding to some of the areas showing maximum concentration of calcium oxalate (bands – 780, 1323 and 1620 cm^{-1}), calcium carbonate (bands – 875, 1420 cm^{-1}) and azurite (bands – 819, 833, 1092, 1417, 1464 and 3429 cm^{-1})

Figure 6: a) µSR-XRD patterns from the layer related to old fungi activity removed from a blue sample. One of the two types of patterns found corresponds to calcium malate dihydrate. b) Backscatter SEM image, µSR-XRD patterns and c) EDS spectra from cross section of an ochre paint; the components of the ochre paint and the superficial fungi activity layer are determined. The presence of gold is related to the sample preparation method used.

Figure 7: Infrared spectra corresponding to the reference LMWOA salts synthesised in our laboratory and prepared in KBr pellets; **a)** Calcium fumarate n-hydrate, **b)** calcium lactate pentahydrate; **c)** calcium succinate n-hydrate and **d)** calcium malate n-hydrate.

Figure 8: a) Series of µSR-FTIR spectra corresponding to the old fungi activity layers obtained from a green paint sample, **b)** 3800-2500 cm^{-1} region and **c)** 1800-600 cm^{-1} region.

Figure 9: µSR-FTIR spectrum from a green paint layer showing the characteristic absorption bands of the hydroxyl stretching vibration of a green earth pigment (celadonite). We can see the overlap with those related to the LMWOAS produced by old fungi activity.

Figure 1.

Figure 2.

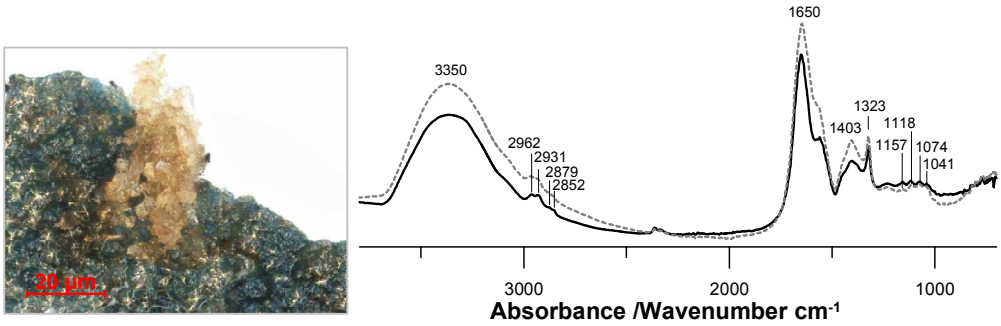
20 µm
3350
2962
2931
2879
2852
1650
1403
1323
1118
1157
1074
1041
3000
2000
1000
Absorbance /Wavenumber cm-1

a b

Figure 3.

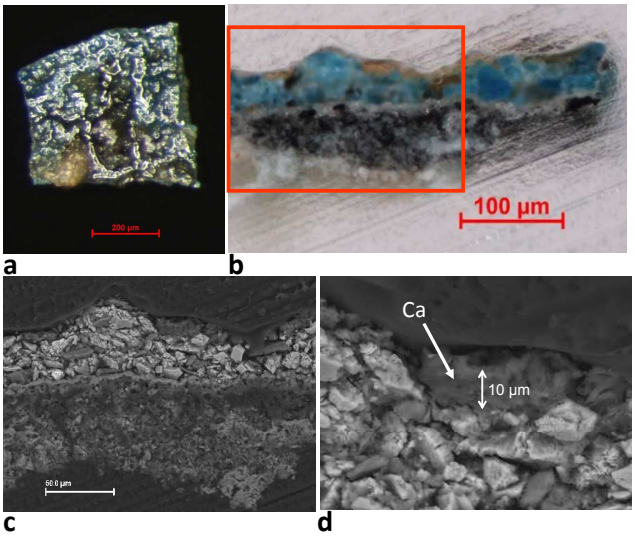

Figure 4.

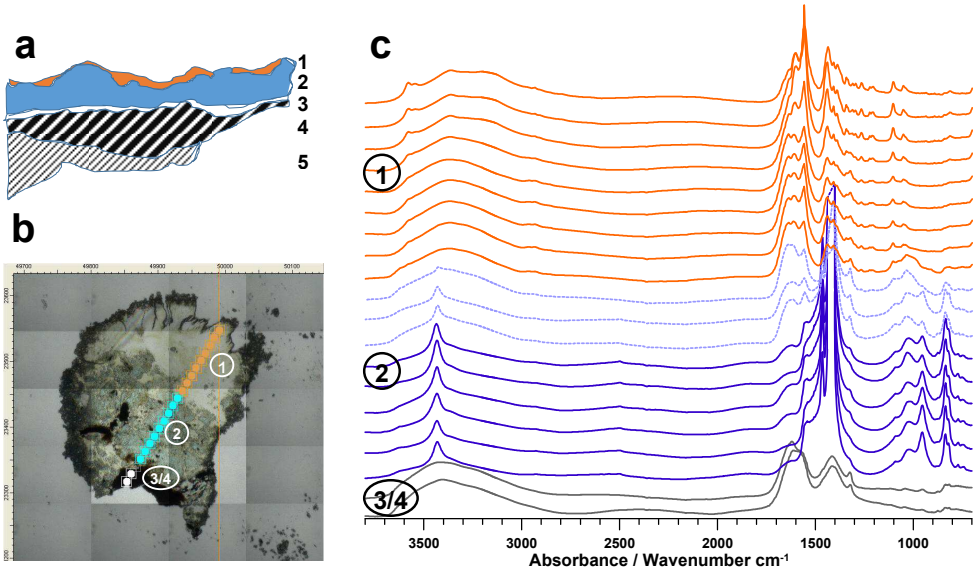
a
1
2
3
4
5
b
1
2
3/4
c
1
2
3/4
3500
3000
2500
2000
1500
1000
Absorbance / Wavenumber cm-1

Figure 5

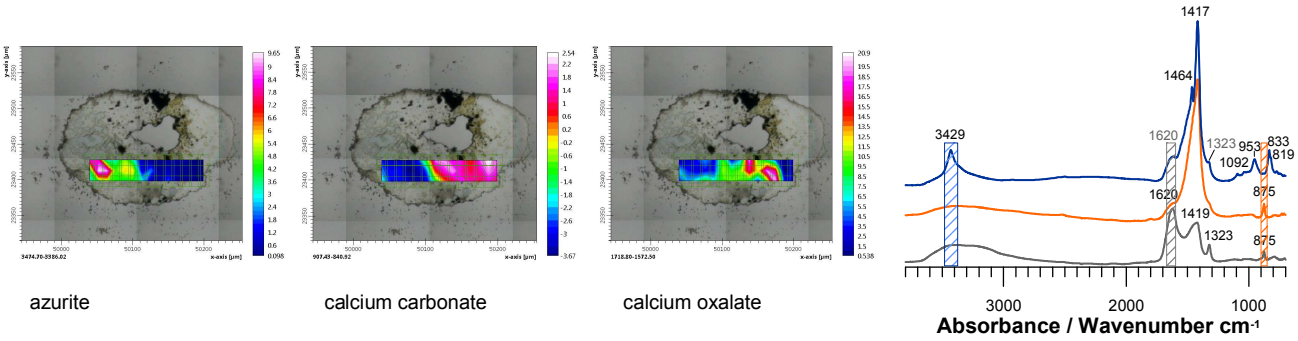

a **b** **c** **d**

Figure 6.

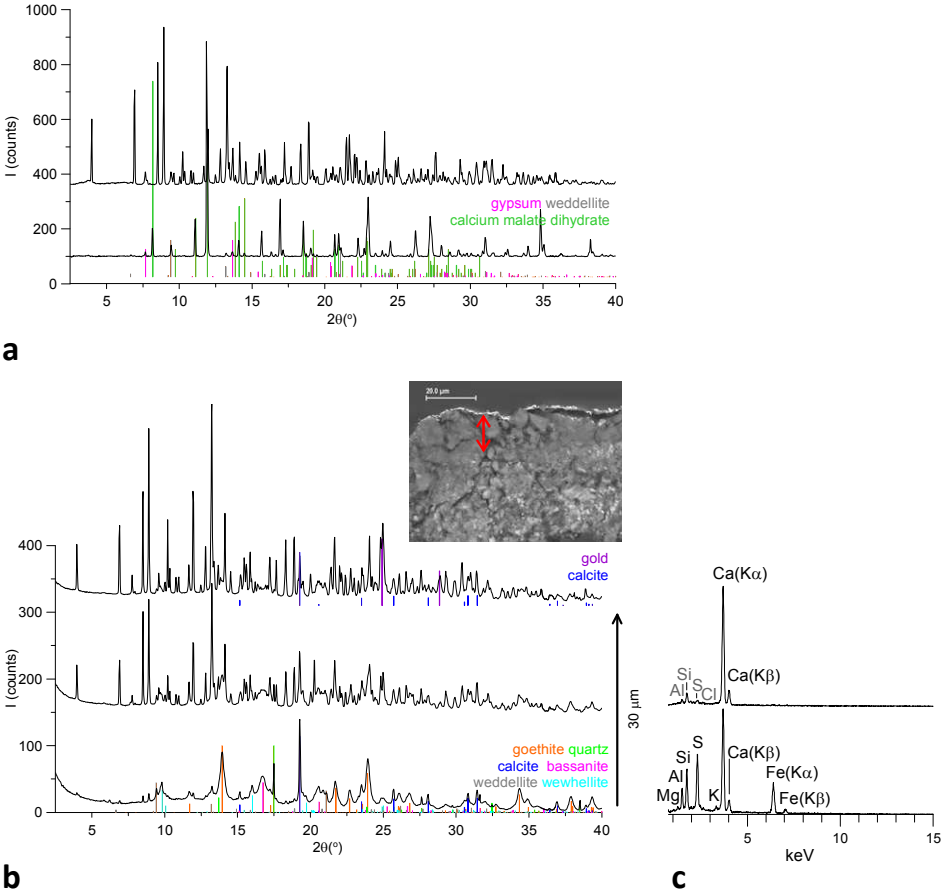
I (counts)
2θ(°)
gypsum weddellite
calcium malate dihydrate
a
gold
calcite
goethite quartz
calcite bassanite
weddellite wewhellite
30 µm
b
Ca(Kα)
Ca(Kβ)
Si
Al
S
Cl
Mg
K
Fe(Kα)
Fe(Kβ)
keV
c

Figure 7

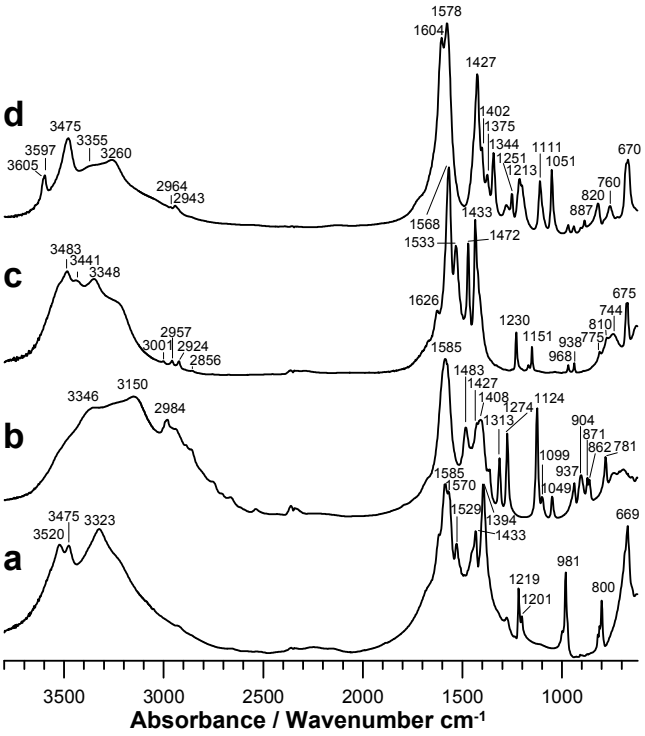
d
c
b
a
1578
1604
1427
1402
1375
1344
1251
1213
1111
1051
670
760
820
887
1433
1472
1568
1533
3475
3355
3597
3605
3260
2964
2943
3483
3441
3348
1626
675
744
810
775
1230
1151
938
968
2957
3001
2924
2856
1585
1483
1427
1408
1274
1124
1313
904
871
862
781
1099
937
1049
3346
3150
2984
1585
1570
1529
1394
1433
669
3475
3520
3323
981
1219
1201
800
3500
3000
2500
2000
1500
1000
Absorbance / Wavenumber cm-1

Figure 8.

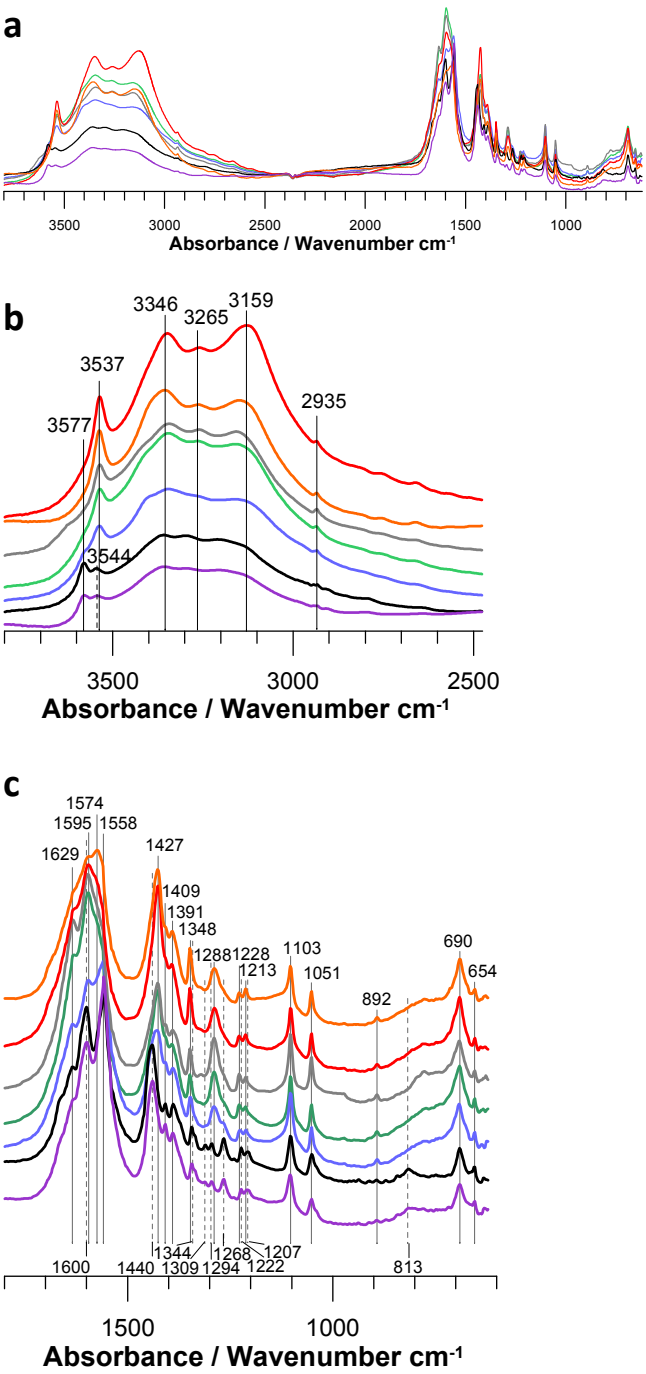
a
3500
3000
2500
2000
1500
1000
Absorbance / Wavenumber cm-1
b
3346
3265
3159
3537
2935
3577
3544
3500
3000
2500
Absorbance / Wavenumber cm-1
c
1574
1595
1558
1629
1427
1409
1391
1348
1288
1228
1213
1103
1051
690
654
892
1344
1268
1207
1600
1440
1309
1294
1222
813
1500
1000
Absorbance / Wavenumber cm-1

Figure 9.

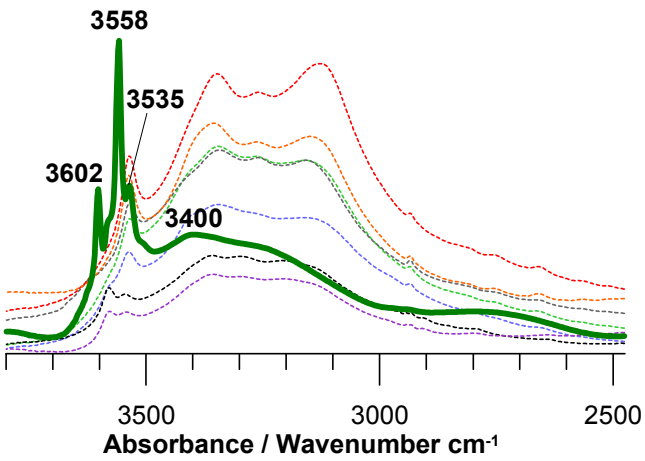
3558
3535
3602
3400
3500
3000
2500
Absorbance / Wavenumber cm-1